



HAL
open science

Gas-Phase Ozone Reaction Kinetics of C-5-C-8 Unsaturated Alcohols of Biogenic Interest

Asma Grira, Cornelia Amarandei, Claudiu Roman, Oumaya Bejaoui, Nouha Aloui, Gisele El Dib, Cecilia Arsene, Iustinian G. Bejan, Romeo I. Olariu, André Canosa, et al.

► **To cite this version:**

Asma Grira, Cornelia Amarandei, Claudiu Roman, Oumaya Bejaoui, Nouha Aloui, et al.. Gas-Phase Ozone Reaction Kinetics of C-5-C-8 Unsaturated Alcohols of Biogenic Interest. *Journal of Physical Chemistry A*, 2022, 126 (27), pp.4413-4423. 10.1021/acs.jpca.2c02805 . hal-03772466

HAL Id: hal-03772466

<https://hal.science/hal-03772466>

Submitted on 17 Oct 2022

HAL is a multi-disciplinary open access archive for the deposit and dissemination of scientific research documents, whether they are published or not. The documents may come from teaching and research institutions in France or abroad, or from public or private research centers.

L'archive ouverte pluridisciplinaire **HAL**, est destinée au dépôt et à la diffusion de documents scientifiques de niveau recherche, publiés ou non, émanant des établissements d'enseignement et de recherche français ou étrangers, des laboratoires publics ou privés.



Distributed under a Creative Commons Attribution - NonCommercial 4.0 International License

1 **Gas-phase ozone reaction kinetics of C₅-C₈ unsaturated alcohols of**
2 **biogenic interest**
3

4 *Asma Grira*^{1,2#}, *Cornelia Amarandei*^{3,4#}, *Claudiu Roman*^{3,4#}, *Oumaya Bejaoui*¹, *Nouha Aloui*¹,
5 *Gisèle El Dib*², *Cecilia Arsene*^{3,4}, *Iustinian G. Bejan*^{3,4}, *Romeo I. Olariu*^{3,4*}, *André Canosa*²,
6 *Alexandre Tomas*^{1,*}
7

8 ¹IMT Nord Europe, Institut Mines-Télécom, Univ. Lille, Center for Energy and Environment,
9 59000 Lille, France
10

11 ²Université de Rennes, CNRS, IPR (Institut de Physique de Rennes), UMR 6251, Rennes, F-
12 35000, France
13

14 ³Faculty of Chemistry, Department of Chemistry, 11 Carol I, “Alexandru Ioan Cuza” University
15 of Iasi, 700506 Iasi, Romania
16

17 ⁴Integrated Centre of Environmental Science Studies in the North Eastern Region, 11 Carol I,
18 “Alexandru Ioan Cuza” University of Iasi, 700506 Iasi, Romania.
19
20
21

22 # first three authors have equal contributions
23

24 *Corresponding authors: alexandre.tomas@imt-nord-europe.fr, +33 327 712 651;
25 oromeo@uaic.ro, +40232201354
26

27 **ABSTRACT**

28 Unsaturated alcohols are volatile organic compounds (VOCs) characterizing the emissions of
29 plants. Changes in climate together with related increases of biotic and abiotic stresses are expected
30 to strengthen these emissions in the future. Ozonolysis of unsaturated alcohols is one of the
31 oxidation pathways that control their fate in the atmosphere. The rate coefficients of gas-phase O₃
32 reaction with seven C₅ to C₈ unsaturated alcohols have been determined at 296 K using both
33 absolute and relative kinetic methods. The following rate coefficients have been obtained (in cm³
34 molecule⁻¹ s⁻¹) from the absolute method: (1.1±0.2)×10⁻¹⁶ for *cis*-2-penten-1-ol, (1.2±0.2)×10⁻¹⁶
35 for *trans*-2-hexen-1-ol, (6.4±1.0)×10⁻¹⁷ for *trans*-3-hexen-1-ol, (5.8±0.9)×10⁻¹⁷ for *cis*-3-hexen-1-
36 ol, (2.0±0.3)×10⁻¹⁷ for 1-octen-3-ol and (8.4±1.3)×10⁻¹⁷ for *trans*-2-octen-1-ol and from the
37 relative method: (1.27±0.11)×10⁻¹⁶ for *trans*-2-hexen-1-ol, (5.01±0.30)×10⁻¹⁷ for *trans*-3-hexen-1-
38 ol, (4.13±0.34)×10⁻¹⁷ for *cis*-3-hexen-1-ol, (1.40±0.12)×10⁻¹⁶ for *trans*-4-hexen-1-ol. Alkenols
39 display high reactivity with ozone with lifetimes in the hour range. Rate coefficients show a strong
40 and complex dependence on the structure of the alkenol, particularly the relative position of the
41 OH group towards the C=C double bond. The results are discussed and compared to the available
42 literature data and four Structure Activity Relationship (SAR) methods.

43

44

45 **KEYWORDS:** unsaturated alcohols, Green Leaf Volatile (GLV), ozonolysis, absolute kinetic
46 method, relative kinetic method, Structure Activity Relationship (SAR) approaches

47

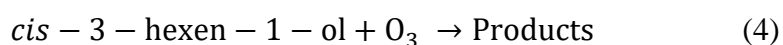
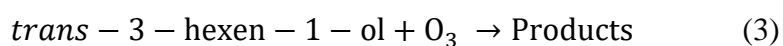
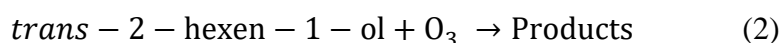
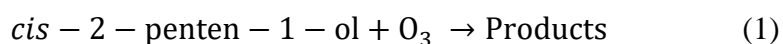
48 **Introduction**

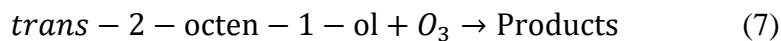
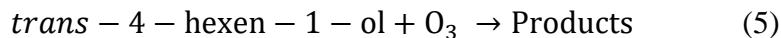
49 It is widely accepted that ozone plays a key role in controlling both atmospheric chemistry and
50 climate change. This is due to its oxidative and light-absorbing properties which present a threat
51 for all the ecosystem elements^{1,2} and to its role in producing hydroxyl (OH) radical which initiates
52 the majority of oxidation processes in the atmosphere³. Therefore, ozone reactivity has been a
53 subject of intensive studies and continues to be of significant concern worldwide. Background
54 ozone concentrations in remote areas are generally within a few $\mu\text{g m}^{-3}$, yet, in many locations,
55 they have been shown to increase steadily in the past decades partly due to increased global
56 emissions of nitrogen oxides (NO_x) and volatile organic compounds (VOCs)⁴⁻⁷.

57 Unsaturated alcohols or alkenols are VOCs emitted by numerous plants due to biological activity
58 (photosynthesis, transpiration...) and cell decomposition⁸. More specifically, C_6 and C_9
59 compounds have been shown to be ubiquitous species characterizing the emissions of plants, with
60 stronger releases under biotic and abiotic stresses with transient emission rates up to 2 orders of
61 magnitude larger than monoterpenes⁹. Once in the atmosphere, the double bond present in the
62 carbon skeleton makes such alcohols quite reactive towards the atmospheric oxidants, thus
63 contributing to the oxidative capacity of the atmosphere. While reactions of unsaturated alcohols
64 with OH radical are relatively well known¹⁰, reactions with ozone have been less investigated and
65 uncertainties remain on their reactivity and atmospheric impact. These latter reactions make
66 unsaturated alcohols relatively short-lived (atmospheric lifetimes around minutes to hours)¹¹ and
67 usually associated with the formation of organic acids¹², organic hydroperoxydes¹³, and secondary
68 organic aerosols¹⁴ (SOA) which often appear as a haze over forests¹⁵.

69 Regarding O₃ + alkenols literature kinetics data, only ambient temperature rate coefficients have
70 been reported. The kinetics of *cis*-2-penten-1-ol was first investigated by Grosjean and Grosjean¹⁶,
71 but the obtained value for the rate coefficient $(1.69 \pm 0.25) \times 10^{-16} \text{ cm}^3 \text{ molecule}^{-1} \text{ s}^{-1}$ is inconsistent
72 with two more recent studies^{14,17} which reported $(1.15 \pm 0.07) \times 10^{-16} \text{ cm}^3 \text{ molecule}^{-1} \text{ s}^{-1}$ and
73 $(1.05 \pm 0.20) \times 10^{-16} \text{ cm}^3 \text{ molecule}^{-1} \text{ s}^{-1}$, respectively. The O₃ kinetics of *trans*-2-hexen-1-ol was
74 recently studied by Gibilisco et al.¹⁸ and Lin et al.¹⁹. The obtained rate coefficients differ by almost
75 a factor of 3, with values of $(0.60 \pm 0.07) \times 10^{-16} \text{ cm}^3 \text{ molecule}^{-1} \text{ s}^{-1}$ and $(1.66 \pm 0.22) \times 10^{-16} \text{ cm}^3$
76 $\text{molecule}^{-1} \text{ s}^{-1}$, respectively. The rate coefficients for the reaction of O₃ with *trans*-3-hexen-1-ol
77 measured by Gibilisco et al.¹⁸, Lin et al.¹⁹ and Kalalian et al.¹⁷ are $(5.83 \pm 0.86) \times 10^{-17}$,
78 $(6.19 \pm 0.72) \times 10^{-17}$ and $(6.24 \pm 1.37) \times 10^{-17} \text{ cm}^3 \text{ molecule}^{-1} \text{ s}^{-1}$, respectively. For *cis*-3-hexen-1-ol,
79 the study of Grosjean et al.²⁰ is about twice higher than those of Atkinson et al.²¹, Gibilisco et al.¹⁸,
80 Lin et al.¹⁹, and Chen et al.²², raising the concern about the kinetic rate coefficients obtained for
81 *cis*-2-penten-1-ol by Grosjean and Grosjean¹⁶. The rate coefficient for the reaction of O₃ with
82 *trans*-4-hexen-1-ol was measured only by Lin et al.¹⁹, who reported $(1.05 \pm 0.21) \times 10^{-16} \text{ cm}^3$
83 $\text{molecule}^{-1} \text{ s}^{-1}$. For 1-octen-3-ol ozonolysis, to the best of our knowledge, only Li et al.²³
84 investigated the kinetics. Table S1 summarizes the above available literature data.

85 The objective of this work was thus to investigate the ozone kinetics of a series of seven
86 unsaturated alcohols from C₅ to C₈:





87 Two complementary experimental setups were implemented using absolute and relative kinetics
88 methods.

89 The results will help resolving the inconsistencies noted above on the rate coefficients and better
90 understand the atmospheric impacts of such compounds in the context of increasing O₃ background
91 concentrations and climate change. Note that this work represents the first investigation of *trans*-
92 2-octen-1-ol + O₃ kinetics. Further, developing structure-activity relationships (SAR) for
93 atmospheric chemistry models needs consistent and extended kinetic databases to which the
94 present work aims to contribute, especially the effect of the position of the double bond with
95 respect to the -OH functional group. Four different SAR approaches proposed in the
96 literature^{24,25,26,27} were tested against alkenols ozonolysis kinetics, including the present results.

97 **Experimental part**

98 *Pseudo first order kinetic set-up (Douai Teflon chamber)*

99 A series of kinetic experiments for *cis*-2-penten-1-ol, *trans*-2-hexen-1-ol, *trans*-3-hexen-1-ol,
100 *cis*-3-hexen-1-ol, 1-octen-3-ol and *trans*-2-octen-1-ol were performed in a Teflon chamber of
101 about 300 L at a temperature of 296±2 K and atmospheric pressure of purified air^{28,29}. This
102 chamber is equipped with inlet and outlet ports used for introducing reactants and taking samples
103 from the reaction mixture. All the connections between the reaction chamber and the instruments
104 were operated via Teflon tubes. Liquid aliquots of alcohols were first vaporized in the chamber
105 under a stream of pure air and the mixture was left to stabilize for ~1h. Preliminary tests were

106 dedicated to the study of alcohol stability in the reactor. Wall losses of alcohols appeared to be
107 negligible in the present conditions (loss rate < 3% per hour for all alcohols). Ozone was produced
108 separately by an O₃ generator (C-Lasky C-010-DTI) based on electrical discharge on pure zero air
109 flow. After stabilization of the alcohol inside the chamber (1σ of three measurements by Fourier
110 Transform Infrared (FTIR) spectroscopy below 3%), a few tens of mL of O₃ were sampled with a
111 gas syringe and added to the reaction mixture under a high flow of air (about 20 L min⁻¹), thus
112 enhancing the prompt mixing of the reactants and starting the reaction.

113 Pseudo-first order conditions were set up with alcohol initial concentrations $[alc]_{t_0}$ ((0.34-
114 3.6)×10¹⁴ molecules cm⁻³) in excess (at least 10 times higher) over that of ozone $[O_3]_{t_0}$ ((1.4-
115 17)×10¹² molecules cm⁻³). The alcohol concentration can thus be assumed to be constant during
116 the experiment. Eq. 1 describes the ozone concentration decay taking into account the ozone wall
117 loss rate (k_w in s⁻¹).

$$-\frac{d[O_3]_t}{dt} = k \times [alc]_{t_0} \times [O_3]_t + k_w \times [O_3]_t \quad (\text{Eq. 1})$$

118 with k the rate coefficient for the reaction between the studied alcohol and O₃ and $[O_3]_t$ is the
119 concentration of ozone at time t . Eq. 1 can be simplified into:

$$-\frac{d[O_3]_t}{dt} = k_{obs} \times [O_3]_t \quad (\text{Eq. 2})$$

120 where $k_{obs} = k \times [alc]_{t_0} + k_w$ is the pseudo-first-order rate constant. Integrating Eq. 2 yields:

$$\ln\left(\frac{[O_3]_{t_0}}{[O_3]_t}\right) = k_{obs} \times t \quad (\text{Eq. 3})$$

121 Plotting $\ln\left(\frac{[O_3]_{t_0}}{[O_3]_t}\right)$ vs t leads to a straight line with zero intercept and a regression coefficient
122 $k_{obs} = k \times [alc]_{t_0} + k_w$. Plotting k_{obs} vs $[alc]_{t_0}$ finally gives the rate coefficient k as the regression
123 coefficient and k_w as the intercept.

124 The ozone decay was monitored by a UV-absorption O₃ analyzer (Environment SA 42M) with
125 a resolution time of 10 s. Preliminary tests showed that the investigated alcohols were not
126 absorbing at the wavelength of the ozone instrument (253.7 nm). Alcohol calibration curves
127 (Figures S1-S6) were carefully determined through FTIR spectroscopy using a 10 m optical length
128 White cell³⁰.

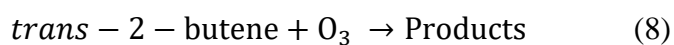
129 Formation of OH radical through the ozonolysis of hexenols was reported by Atkinson et al.²¹
130 (OH yield of about 26%). No OH scavenger was used in the Douai Teflon chamber, except for 1-
131 octen-3-ol where two experiments were performed with excess of cyclohexane (200 and 1000
132 ppm). In these two experiments, about 90% of the OH were scavenged by cyclohexane. It should
133 be stressed, however, that any OH radical formed will react with the alcohol but would not affect
134 the ozone decay in a significant manner at the high initial alcohol/ozone concentration ratios
135 employed. The two experiments noted above were carried out to confirm the absence of effect on
136 the O₃ decay.

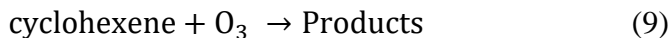
137 Primary products from reactions of unsaturated compounds with O₃ are mainly carbonyls³¹.
138 Potential interferences from these carbonyls in the O₃ analyzer are expected to be negligible since
139 the absorption cross section ratios between ozone and carbonyls at 253.7 nm (detection wavelength
140 of the O₃ analyzer) are in the range of 400 to 4000³². Hence, carbonyl absorption will be negligible
141 compared to that of ozone. Consistently, Peters et al.³³ found no interferences for commercial
142 ozone monitor for a series of VOCs including alcohols and carbonyls.

143 Concentrations of *cis*-2-penten-1-ol, *trans*-2-hexen-1-ol, *trans*-3-hexen-1-ol, *cis*-3-hexen-1-ol,
144 1-octen-3-ol and *trans*-2-octen-1-ol were measured in the following IR ranges, respectively: 960-
145 1081 cm⁻¹, 956-1032 cm⁻¹, 934-1000 cm⁻¹, 997-1096 cm⁻¹, 913-940 cm⁻¹, and 900-1050 cm⁻¹.

146 *Relative rate kinetic set-up (Iasi ESC-Q-UAIC reaction chamber)*

147 A series of kinetic experiments for *trans*-2-hexene-1-ol, *trans*-3-hexen-1-ol, *cis*-3-hexen-1-ol,
148 and *trans*-4-hexene-1-ol were performed at 298 K and 1 atm of air pressure, using the facilities of
149 the Environmental Simulation Chamber made out of Quartz from “Alexandru Ioan Cuza”
150 University of Iasi (ESC-Q-UAIC), Romania. The reactor consists of three quartz tubes with a total
151 length of 4.1 m and a total volume of 760 L. The homogeneous mixture of compounds inside the
152 reactor is achieved by two Teflon fans. The reactor can be evacuated down to 10^{-2} mbar. Both ends
153 are closed with anodized aluminum flanges and are provided with multiple inlet and outlet ports.
154 A Bruker Vertex 80 FT-IR spectrometer was used for collecting IR spectra over a White type
155 mirror system with an optical path length of 492 m at a resolution of 1 cm^{-1} . A more detailed
156 description of the reactor can be found in literature³⁴. The relative kinetics method was employed
157 for rate coefficient measurements using *trans*-2-butene and cyclohexene as reference compounds
158 with $k(\textit{trans}\text{-2-butene}+\text{O}_3) = (2.00\pm 0.50)\times 10^{-17}\text{ cm}^3\text{ molecule}^{-1}\text{ s}^{-1}$ ³⁵ and $k(\text{cyclohexene}+\text{O}_3) =$
159 $(7.44\pm 1.86)\times 10^{-17}\text{ cm}^3\text{ molecule}^{-1}\text{ s}^{-1}$ ³⁶. 1,3,5-Trimethylbenzene was used as OH scavenger in
160 concentrations such that more than 90% of any OH radicals produced was suppressed during the
161 ozonolysis of unsaturated compounds. For *trans*-3-hexene-1-ol only, two other additional
162 scavengers were employed: cyclohexane and di-butyl ether. The reason was to check whether or
163 not the nature of the scavengers plays any role in this study. Preliminary tests to measure wall
164 depositions of *trans*-2-hexene-1-ol, *trans*-3-hexen-1-ol, *cis*-3-hexen-1-ol, and *trans*-4-hexene-1-ol
165 revealed the following wall loss rates (k_{WL}): $(4.93\pm 0.45)\times 10^{-5}\text{ s}^{-1}$, $(4.35\pm 0.50)\times 10^{-5}\text{ s}^{-1}$,
166 $(5.08\pm 0.51)\times 10^{-5}\text{ s}^{-1}$ and $(6.04\pm 0.53)\times 10^{-5}\text{ s}^{-1}$, respectively. No wall deposition was observed for
167 the reference compounds. In the gas-phase system, besides the reaction of alkenols with ozone,
168 reference compounds would also react with ozone (reactions (8) and (9)):





169 For the unsaturated alcohols and reference compounds the following kinetic equations are valid
 170 in the relative method approach:

$$-\frac{d[alc]_t}{dt} = k \times [alc]_t \times [O_3]_t + k_{WL} \times [alc]_t \quad (\text{Eq. 4})$$

$$-\frac{d[reference]_t}{dt} = k_{ref} \times [reference]_t \times [O_3]_t \quad (\text{Eq. 5})$$

171 where $[alc]_t$ and $[reference]_t$ are the concentrations of the alcohols and reference compounds
 172 at time t. Integrating and combining these two equations yields the following relation between the
 173 alcohols and reference concentrations and the O_3 reaction rate coefficients:

$$\ln \frac{[alc]_{t_0}}{[alc]_t} - k_{WL} \times (t - t_0) = \frac{k}{k_{ref}} \ln \frac{[reference]_{t_0}}{[reference]_t} \quad (\text{Eq. 6})$$

174 where $[alc]_{t_0}$ and $[reference]_{t_0}$ are the initial concentrations of unsaturated alcohols and
 175 reference compounds, k and k_{ref} are the rate coefficients of the reaction of alcohols and reference
 176 compounds with ozone.

177 The initial concentrations were estimated based on the weighted amounts injected into the
 178 reaction chamber, as the difference of the syringe weights with the liquid compound and without
 179 liquid compound measured right after the injection, leading to the following average values (in
 180 molecules cm^{-3} , where the uncertainties are two standard deviations): $(7.37 \pm 0.39) \times 10^{13}$ for
 181 alcohols, $(8.12 \pm 1.62) \times 10^{13}$ for *trans*-2-butene, $(4.69 \pm 0.78) \times 10^{13}$ for cyclohexene. Regarding OH
 182 scavengers, their concentrations (in molecules cm^{-3}) were calculated based on the volume injected:
 183 2.30×10^{15} for 1,3,5-trimethylbenzene, 3.00×10^{16} for cyclohexane and 5.60×10^{15} for di-butyl ether.
 184 The OH scavenger concentration was estimated to suppress up to 90% of OH radicals considering

185 the initial concentrations of the alcohols and reference compounds and their reactivity toward OH
186 radicals³⁷.

187 The target alcohols, references and OH scavengers were obtained commercially with the
188 following purities: *cis*-2-penten-1-ol (Aldrich, > 96%), *trans*-2-hexen-1-ol (Aldrich, ≥ 95%),
189 *trans*-3-hexen-1-ol (Aldrich, 97%), *cis*-3-hexen-1-ol (Fluka, > 98%), 1-octen-3-ol (Aldrich, ≥
190 98%), *trans*-2-octen-1-ol (Aldrich, 97%), *trans*-4-hexen-1-ol (Aldrich, 97%), *trans*-2-butene
191 (Aldrich, 99%), cyclohexene (Aldrich, 99%), 1,3,5-trimethylbenzene (Aldrich, 98%), cyclohexane
192 (Carl-Roth, > 99.5%), di-butyl ether (Aldrich, 99.3%). They were used as received without further
193 purification. At Iasi ESC-Q-UAIC, synthetic air (Messer-Griesheim, 99.999%) and oxygen
194 (Messer-Griesheim, 99.999%) were used while ozone was produced photochemically by passing
195 a flow of O₂ over a VUV-Hg lamp mounted inside a tube and connected to the reactor. Extra pure
196 zero air was produced in Douai with pure air generator (Claind AZ 2020) with relative humidity
197 RH < 2 ppm, CO and CO₂ < 80 ppb.

198 **Results and discussion**

199 *Rate coefficients*

200 An example of pseudo-first order kinetic plots representing k_{obs} as a function of $[alc]_{t_0}$ is
201 displayed in Figure 1 for *trans*-2-octen-1-ol. The kinetic plots for the other 5 alkenols are provided
202 in Supporting Information (Figures S7-S11). All plots show very good linearity with close to zero
203 intercepts. The ozone rate coefficients obtained from the slope of these plots are (in 10⁻¹⁷ cm³
204 molecule⁻¹ s⁻¹): 11.0±2.0 for *cis*-2-penten-1-ol, 12.0±2.0 for *trans*-2-hexen-1-ol, 6.4±1.0 for *trans*-
205 3-hexen-1-ol, 5.8±0.9 for *cis*-3-hexen-1-ol, 2.0±0.3 for 1-octen-3-ol and 8.4±1.3 for *trans*-2-octen-
206 1-ol. Quoted uncertainties are two standard deviations and represent the statistical error on the
207 ozone decays (about 5%) combined with the uncertainty coming from alcohol concentrations (of

208 about 15%, both statistical and systematic errors). The final uncertainty on k , $\Delta(k)$, was calculated
209 using the error propagation method through Eq. 7 and is about 16% for each rate coefficient.

$$\frac{\Delta(k)}{k} = \sqrt{\left(\frac{\Delta k_{obs}}{k_{obs}}\right)^2 + \left(\frac{\Delta[alc]_{t_0}}{[alc]_{t_0}}\right)^2} \quad (\text{Eq. 7})$$

210 Studies performed in Iasi by using the relative kinetic method measured simultaneously the
211 reference decay and the degradation of hexenols during the ozonolysis. The total measured decay
212 of hexenols during the experiments was counted from 20% to 35% (about 48% for O_3) from which
213 $(91.0 \pm 3.3)\%$ of *trans*-2-hexen-1-ol, $(91.5 \pm 7.8)\%$ of *trans*-3-hexen-1-ol, $(83.4 \pm 4.6)\%$ of *cis*-3-
214 hexen-1-ol and $(91.4 \pm 1.8)\%$ of *trans*-4-hexen-1-ol reacted with ozone. Fairly linear distributions
215 of the data points on the kinetic slopes can be observed in Figure 2 (*trans*-2-hexen-1-ol) and
216 Figures S12-S14 (*trans*-3-hexen-1-ol, *cis*-3-hexen-1-ol, and *trans*-4-hexen-1-ol) in Supplementary
217 Information. Table 1 reports the experimental results obtained from the relative kinetic
218 investigations. The ratios between rate coefficients of hexenols and reference compounds (k/k_{ref})
219 and the attributed uncertainties (2σ) were retrieved from linear regression analysis. Uncertainties
220 for k values were obtained by propagating 10% error from the k_{ref} values and 2σ from the slope of
221 our experimental data. The value of k (average) and its associated uncertainty is derived from the
222 weighted average for k values. The control test experiment (relative kinetics between *trans*-2-
223 butene and cyclohexene) presented in Supplementary Information (Figure S15) shows a maximum
224 of 5% difference between the measured and literature rate coefficients ratios ($k_{cyclohexene+O_3}/k_{trans-2-}$
225 *butene+O_3*), this slight difference being covered by the proposed uncertainties. One could notice the
226 very good agreement between the O_3 rate coefficients obtained for *trans*-3-hexen-1-ol when three
227 different OH radical scavengers were used. These results proved that the effect of OH radical could
228 be suppressed by using any of the scavengers.

229 Table 2 compares the rate coefficients obtained in the present work (absolute and relative
230 methods) with literature data, where available. The rate coefficient obtained for *cis*-2-penten-1-ol
231 $((1.1\pm 0.2)\times 10^{-16} \text{ cm}^3 \text{ molecule}^{-1} \text{ s}^{-1})$ is in excellent agreement with the determinations of O'Dwyer
232 et al.¹⁴ and Kalalian et al.¹⁷ who found $(1.15\pm 0.07)\times 10^{-16} \text{ cm}^3 \text{ molecule}^{-1} \text{ s}^{-1}$ and $(1.05\pm 0.20)\times 10^{-16}$
233 $\text{ cm}^3 \text{ molecule}^{-1} \text{ s}^{-1}$, respectively, while about 33% lower than the study from Grosjean and
234 Grosjean¹⁶ of $(1.69\pm 0.25)\times 10^{-16} \text{ cm}^3 \text{ molecule}^{-1} \text{ s}^{-1}$. All previous literature studies used the absolute
235 kinetics method except Kalalian et al.¹⁷, who used the relative method. Grosjean and Grosjean¹⁶
236 carried out only three experiments under 55% relative humidity using cyclohexane as scavenger
237 with no variation of the initial alkenol concentration, leading to probably less reliable results. A
238 higher rate coefficient value may also point to unknown secondary losses such as impurities in *cis*-
239 2-penten-1-ol. Yet, with a stated purity of 99%,¹⁶ the 1% impurity should have reacted with O₃ at
240 a fairly high rate coefficient of about $5\times 10^{-15} \text{ cm}^3 \text{ molecule}^{-1} \text{ s}^{-1}$ in order to yield the 30% higher
241 *cis*-2-penten-1-ol + O₃ rate coefficient measured by Grosjean and Grosjean¹⁶. Reactions of Criegee
242 Intermediates (CI) with alkenols may also be evoked as potential additional loss of alkenols. In the
243 absence of kinetics data, an alkenol + CI rate coefficient of about $1\times 10^{-13} \text{ cm}^3 \text{ molecule}^{-1} \text{ s}^{-1}$ can
244 be estimated based on the reactivity of CI with alkenes³⁸ and alcohols³⁹. The comparison of the
245 rate of alkenol + O₃ ($r_{\text{O}_3} = k\times [\text{O}_3]\times [\text{alc}]$, with $k = 1.1\times 10^{-16} \text{ cm}^3 \text{ molecule}^{-1} \text{ s}^{-1}$ in the case of *cis*-2-
246 penten-1-ol and $[\text{O}_3] = 1\times 10^{12} \text{ molecules cm}^{-3}$) with the estimated rate of alkenol + CI ($r_{\text{CI}} =$
247 $k_{\text{CI}}\times [\text{CI}]\times [\text{alc}]$ with $k_{\text{CI}} = 1\times 10^{-13} \text{ cm}^3 \text{ molecule}^{-1} \text{ s}^{-1}$ and $[\text{CI}]$ estimated at $1\times 10^6 \text{ molecules cm}^{-3}$)
248 leads to a ratio of about 1000. This value indicates that alkenol reactions with CI are probably not
249 significant in the present chamber experiments. Hence, the possible discrepancies in the rate
250 constants between the present work and literature values cannot be explained by CI reactions with
251 alkenols.

252 For *trans*-2-hexen-1-ol, a rate coefficient of $(1.2\pm 0.2)\times 10^{-16}$ cm³ molecule⁻¹ s⁻¹ was obtained by
253 the absolute kinetic method and $(1.27\pm 0.11)\times 10^{-16}$ cm³ molecule⁻¹ s⁻¹ by the relative rate kinetic
254 approach. Both investigations are virtually similar and are in good agreement with the last study
255 by Lin et al.¹⁹ ($(1.66\pm 0.22)\times 10^{-16}$ cm³ molecule⁻¹ s⁻¹) while significantly larger (about a factor of
256 two) than Gibilisco et al.¹⁸ who found $(5.98\pm 0.73)\times 10^{-17}$ cm³ molecule⁻¹ s⁻¹. However, in this latter
257 study, it was mentioned that OH radicals were not sufficiently scavenged and the results should be
258 considered with caution. Gibilisco et al.¹⁸ corrected the obtained rate coefficients by inclusion of
259 self-canceling terms of $-k_{\text{hexenol}}[\text{OH}]dt$ and $-k_{\text{reference}}[\text{OH}]dt$ based on the assumption that
260 references have identical rate coefficients against ozone and similar OH radical yields of 26% as
261 reported for isoprene and *trans*-3-hexen-1-ol.

262 For *trans*-3-hexen-1-ol and *cis*-3-hexen-1-ol where the double bond is further from the -OH
263 group compared to *trans*-2-hexen-1-ol, lower rate coefficients are obtained in the present work,
264 $(6.4\pm 1.0)\times 10^{-17}$ and $(5.8\pm 0.9)\times 10^{-17}$ cm³ molecule⁻¹ s⁻¹, respectively, when employing the pseudo-
265 first order kinetic method and $(5.01\pm 0.30)\times 10^{-17}$ and $(4.13\pm 0.34)\times 10^{-17}$ cm³ molecule⁻¹ s⁻¹ when
266 using relative rate kinetics. Experimental evidence for other unsaturated alcohols^{14,40} as well as
267 quantum chemistry calculations¹⁹ supports a higher rate coefficient when the double bond is in α
268 position with respect to the -OH functional group, as is the case with *trans*-2-hexen-1-ol. It should
269 be noted that both 3-hexen-1-ol isomers (*cis*- and *trans*-) display a relatively similar reactivity
270 towards O₃, while literature reviews on alkene + O₃ kinetics indicate that *trans*- isomers are
271 generally more reactive than *cis*- due to a higher pre-exponential factor^{41,42}. Consistently, a slightly
272 higher rate coefficient value can be observed for the *trans*- isomer in comparison with the *cis*-
273 isomer, though this conclusion could be encompassed if the uncertainties level is considered. It is
274 important to mention that rate coefficient values obtained for 3-hexen-1-ol isomers agree within

275 30% with the literature values obtained by using different methods and simulation chambers as
276 those used in present investigations (see Table 2). However, most of the difference could be
277 explained considering the assumed errors of about 20% of the reference rate coefficients used in
278 the relative rate method. As for *cis*-2-penten-1-ol, only three experiments were performed by
279 Grosjean et al.²⁰ for *cis*-3-hexen-1-ol with no variation of the initial alkenol concentration. This
280 may explain the discrepancies observed for $k_{cis-3-hexen-1-ol+O_3}$ between Grosjean et al.²⁰, on the one
281 hand, and the other studies (including the present work), on the other hand.

282 The kinetic values for *trans*-4-hexen-1-ol (in $\text{cm}^3 \text{ molecule}^{-1} \text{ s}^{-1}$) are in good agreement for both
283 reference compounds ($(14.1 \pm 1.7) \times 10^{-17}$ with *trans*-2-butene and $(13.9 \pm 1.8) \times 10^{-17}$ with
284 cyclohexene) and with Lin et al.¹⁹ ($(10.5 \pm 1.4) \times 10^{-17}$) considering the uncertainties. In an attempt
285 to compare the rate coefficient of *trans*-2-hexen-1-ol, *trans*-3-hexen-1-ol and *trans*-4-hexen-1-ol,
286 a virtually similar reactivity for *trans*-2-hexen-1-ol and *trans*-4-hexen-1-ol is observed while the
287 rate coefficient for *trans*-3-hexen-1-ol is about three times lower.

288 For 1-octen-3-ol, our value is in excellent agreement with the only literature data from Li et al.²³.
289 Finally, the present work reports the first O₃ rate coefficient for *trans*-2-octen-1-ol.

290 As observed in many studies on alkenes + O₃ reaction kinetics^{43,44}, a higher degree of alkyl
291 substitution of the double bond generally leads to a higher rate coefficient. Considering all rate
292 coefficients known for alkenols + O₃ (Table S1) suggests that it is also the case for alkenols. Note
293 that the highest *k* value is for 3-methyl-2-buten-1-ol ($> 4.39 \times 10^{-16} \text{ cm}^3 \text{ molecule}^{-1} \text{ s}^{-1}$) which is a
294 tri-substituted compound. This phenomenon has been explained by an inductive effect produced
295 via the enhancement of the π -orbital electron density for higher substituted compounds, leading to
296 a lowering of the activation energy.

297 In the case of unsaturated compounds, the hydroxyl function group is expected to induce an
298 electron-donating effect on the adjacent bonds, thus enhancing the electronic density of the double
299 bond and increasing the reactivity of the unsaturated compound. Comparing the O₃ reactivity of
300 alkenols with that of the corresponding alkenes as a function of the distance between –OH and
301 C=C displays a puzzling picture, as shown in Figure 3. While for 1-alken-3-ols, the rate coefficient
302 ratio $k(\text{O}_3+\text{alkenol})/k(\text{O}_3+\text{alkene})$ is higher than 1, as expected, the reverse is observed for all other
303 alkenols. The highest ratio of about 2 is calculated for 1-octen-3-ol/1-octene and 1-nonen-3-ol/1-
304 nonene. Mason et al. showed that C₃ to C₁₀ 1-alkenes all react with O₃ with rate coefficients around
305 $1 \times 10^{-17} \text{ cm}^3 \text{ molecule}^{-1} \text{ s}^{-1}$ without any effect of the carbon chain length⁴⁵. Interestingly, the present
306 results indicate that the substitution by OH at the α -position to the C=C bond in 1-alkenes increases
307 the rate coefficient up to a factor two. In addition to the electron-donating effect of the –OH group,
308 this may be due to the formation of a strong pre-reactive complex through hydrogen bond
309 interaction between O₃ and –OH¹⁹. Noteworthy, 2-alken-1-ols like 2-penten-1-ol (which are α -
310 alkenols) do not show such reactivity increase between alkenes and alkenols, probably due to steric
311 effects. Further experimental and theoretical investigations of reaction mechanisms of α -alkenols
312 + O₃ may help understanding their reactivity.

313 *Structure-Activity Relationships (SAR)*

314 Rate coefficients can be estimated using different methods involving structure reactivity
315 relationships. Atkinson and Carter²⁴ applied a methodology used by the US Environmental
316 Protection Agency under the AOPWIN (Atmospheric Oxidation Program for Windows) to
317 estimate ozone rate coefficients. Calvert et al.²⁵ developed SAR methods using the group-
318 additivity approach and factors contributions. Pfrang et al.²⁶ used correlations and rate coefficients
319 for basic structures multiplied by group reactivity factors for corresponding substituents. More

320 recently, a new SAR method was developed implying the contribution of inductive effect of
321 heteroatoms and total steric effects based on the earlier work of McGillen et al.⁴⁶ on alkenes and
322 extended by McGillen et al.²⁷ to heteroatomic unsaturated VOCs.

323 The different SAR approaches cited above were applied to evaluate their suitability as alternative
324 tools for rate coefficient estimation for the reactions of unsaturated alcohols with ozone. Where
325 applicable, the experimental values were calculated by averaging rate coefficients obtained in the
326 present work by the pseudo-first order approach and the relative rate kinetic method. In Table 3,
327 the experimental k values (k_{exp}) can be compared with the calculated values obtained using the
328 different SAR approaches (k_{SAR}) on the investigated compounds. The earliest methodologies
329 proposed in the literature on SAR estimations of rate coefficients show large discrepancies with
330 the experimental results. Poor agreement was also noticed when using the SAR approach from
331 Pfrang et al.²⁶ (except for 3-hexen-1-ol isomers) despite the more complex methodology involved.
332 Using McGillen et al.²⁷ methodology (details are provided in the Supplementary Information), a
333 very satisfactory estimate is obtained for *cis*-2-penten-1-ol, *trans*-2-hexen-1-ol and *trans*-2-octen-
334 1-ol, with agreement with our results between 2% and 20%. For the others alkenols, the ratios
335 $k_{\text{SAR}}/k_{\text{exp}}$ vary between 0.29 and 0.59. The strongest disagreement is obtained for *trans*-4-hexen-
336 1-ol ($k_{\text{SAR}}/k_{\text{exp}} = 0.29$) for which the experimental finding is three times larger than the calculated
337 rate coefficient. Because of the distance between -OH and C=C in *trans*-4-hexen-1-ol (-OH is in
338 δ position towards C=C), no inductive effect is considered in the SAR calculation. Consistently,
339 the experimental rate coefficient of the corresponding alkene (*trans*-2-hexene) with O₃ (1.53×10^{-16}
340 $\text{cm}^3 \text{ molecule}^{-1} \text{ s}^{-1}$)³⁷ is close to that obtained in the present work for *trans*-4-hexen-1-ol (1.40×10^{-16}
341 $\text{cm}^3 \text{ molecule}^{-1} \text{ s}^{-1}$). Therefore, the low $k_{\text{SAR}}/k_{\text{exp}}$ ratio reflects a weakness in the SAR method,
342 probably regarding a change in the reaction mechanisms as suggested by McGillen et al.²⁷. Based

343 on the overall agreement, it is suggested that the SAR method from McGillen et al.²⁷ estimates the
344 rate coefficients from ozonolysis of unsaturated alcohols much closer to the experimental data than
345 the other above-mentioned approaches.

346 Ozonolysis rate coefficients were also computed for a range of other alkenols using the SAR
347 method from McGillen et al.²⁷. Values are reported in Figure 4 as a function of experimental ones
348 (see Table S1). Besides the compounds already included in McGillen et al.²⁷ analysis (with updated
349 values from Kalalian et al.¹⁷ and the present work), fourteen new compounds were added (see
350 Table S1, compounds in italic). It can be seen that calculated rate coefficients are within a factor
351 of 2 of the experimental rate coefficients. A linear regression (forced through zero) on the data
352 yields a slope coefficient of 0.64 ± 0.11 (2σ uncertainty), indicating that SAR calculated rate
353 coefficients are mostly lower than experimental ones. As stressed above, this may suggest
354 unknown changes in reaction mechanisms of alkenol ozonolysis. Additional experiments are
355 clearly needed to better characterize these mechanisms and improve structure activity
356 relationships.

357 **Atmospheric implications**

358 The rate coefficients determined in the present work allow calculating the lifetime τ of alkenols
359 in the atmosphere when reacting with O_3 , using $\tau = 1/(k \times [O_3])$. Assuming an average ozone
360 concentration of 1.6×10^{12} molecules cm^{-3} (about 65 ppb at 295 K and 1 atm)⁴⁷ leads to lifetimes
361 of a few hours (Table 4). The corresponding lifetimes when reacting with OH, NO_3 and Cl can be
362 similarly calculated and are reported also in Table 4. Comparing with OH, NO_3 and Cl reactions
363 indicates that ozonolysis is a competitive oxidation process, especially during the night and at low
364 NO_x environments where OH and NO_3 concentrations are low, respectively. In addition, in the

365 perspective of increasing ozone concentrations in the future⁴⁸, an increasing impact of ozonolysis
366 may be expected in the degradation of alkenols.

367 **Conclusions**

368 The rate coefficients of a series of seven unsaturated alcohols with ozone have been determined
369 using two complementary setups, allowing both absolute and relative kinetics methods to be
370 employed. Good agreement has been obtained between the two methods. Alkenols appear to have
371 high reactivity with ozone with lifetime in the hour range. Rate coefficients show a strong and
372 complex dependence on the structure of the alkenol, particularly the relative position of the OH
373 group towards the C=C double bond. Four SAR approaches were tested against the investigated
374 compounds, the most recent from McGillen et al.²⁷ displaying the best results. Yet, efforts are still
375 needed to better understand the reaction mechanisms and unravel the links between the structure
376 and the reactivity of alkenols with O₃.

377 **Supporting Information**

378 Details for evaluating SAR rate coefficients using McGillen et al.²⁷ methodology, ambient
379 temperature ozonolysis rate coefficients of alkenols (Table S1), IR calibration curves for
380 unsaturated alcohols with the corresponding integrated band intensities (IBI, Figures S1-S6),
381 kinetic plots from the absolute and relative rate methods (Figures S7-S14), relative kinetic plot of
382 ozone reaction with *trans*-2-butene vs cyclohexene, (data obtained from control experiments in
383 ESC-Q-UAIC chamber; 1,3,5-trimethylbenzene was used as OH scavenger) (Figure S15).

384 **Acknowledgements**

385 The Center for Energy and Environment acknowledges funding by the French ANR Agency
386 under contract No. ANR-11-LabX-0005-01 CaPPA (Chemical and Physical Properties of the
387 Atmosphere), the Région Hauts-de-France, the Ministère de l'Enseignement Supérieur et de la

388 Recherche (CPER Climibio), and the European Fund for Regional Economic Development. AG
389 is grateful for a PhD grant from Brittany Region and IMT Nord Europe. AG, GED, AC and AT
390 are grateful to the INSU-LEFE-CHAT program for funding this research. CAr, IGB, RIO and AT
391 acknowledge the financial support from European Union's Horizon 2020 Research and Innovation
392 Framework Program, through the EUROCHAMP-2020 Infrastructure Activity Grant (grant
393 agreement No 730997). CAr, IGB, RIO, CA_m and CR and acknowledge the Operational Program
394 Competitiveness 2014-2020, Axis 1, under POC / 448 / 1 / 1 Research infrastructure projects for
395 public R&D institutions / Sections F 2018, through the Research Center with Integrated
396 Techniques for Atmospheric Aerosol Investigation in Romania (RECENT AIR) project, under
397 grant agreement MySMIS no. 127324 for its co-support. All the authors are thankful to the PHC
398 Brancusi program for funding the OzOA project (38385UD).

399 **References**

- 400 (1) Reich, P. B. Quantifying Plant Response to Ozone: A Unifying Theory. *Tree Physiol.* **1987**,
401 3 (1), 63–91.
- 402 (2) Scabba, F.; Giuntini, D.; Castagna, A.; Soldatini, G.; Ranieri, A. Analysing the Impact of
403 Ozone on Biochemical and Physiological Variables in Plant Species Belonging to Natural
404 Ecosystems. *Environ. Exp. Bot.* **2006**, 57 (1–2), 89–97.
- 405 (3) Finlayson-Pitts, B. J.; Pitts, J. N. Atmospheric Chemistry of Tropospheric Ozone Formation:
406 Scientific and Regulatory Implications. *Air Waste* **1993**, 43 (8), 1091–1100.
- 407 (4) Bortz, S. E.; Prather, M. J.; Cammas, J.-P.; Thouret, V.; Smit, H. Ozone, Water Vapor, and
408 Temperature in the Upper Tropical Troposphere: Variations over a Decade of MOZAIC
409 Measurements. *J. Geophys. Res.* **2006**, 111 (D5), D05305. .
- 410 (5) Sicard, P.; Serra, R.; Rossello, P. Spatiotemporal Trends in Ground-Level Ozone
411 Concentrations and Metrics in France over the Time Period 1999–2012. *Environ. Res.* **2016**,
412 149, 122–144.
- 413 (6) Jenkin, M. E. Trends in Ozone Concentration Distributions in the UK since 1990: Local,
414 Regional and Global Influences. *Atmos. Environ.* **2008**, 42 (21), 5434–5445.
- 415 (7) Cooper, O. R.; Schultz, M. G.; Schröder, S.; Chang, K.-L.; Gaudel, A.; Benítez, G. C.;
416 Cuevas, E.; Fröhlich, M.; Galbally, I. E.; Molloy, S. et al., Multi-Decadal Surface Ozone
417 Trends at Globally Distributed Remote Locations. *Elem. Sci. Anthr.* **2020**, 8, 23.
- 418 (8) Kleist, E.; Mentel, T. F.; Andres, S.; Bohne, A.; Folkers, A.; Kiendler-Scharr, A.; Rudich,
419 Y.; Springer, M.; Tillmann, R.; Wildt, J. Irreversible Impacts of Heat on the Emissions of
420 Monoterpenes, Sesquiterpenes, Phenolic BVOC and Green Leaf Volatiles from Several
421 Tree Species. *Biogeosciences* **2012**, 9 (12), 5111–5123.

- 422 (9) Heiden, A. C.; Kobel, K.; Langebartels, C.; Schuh-Thomas, G.; Wildt, J. Emissions of
423 Oxygenated Volatile Organic Compounds from Plants Part I: Emissions from Lipoxygenase
424 Activity. *J. Atmospheric Chem.* **2003**, *45* (2), 143–172.
- 425 (10) Calvert, J. G.; Mellouki, A.; Orlando, J. J.; Pilling, M. J.; Wallington, T. J. *Mechanisms of*
426 *Atmospheric Oxidation of the Oxygenates*; Oxford University Press, 2011.
- 427 (11) Atkinson, R. Gas-Phase Tropospheric Chemistry of Volatile Organic Compounds: 1.
428 Alkanes and Alkenes. *J. Phys. Chem. Ref. Data* **1997**, *26* (2), 215–290.
- 429 (12) Horie, O.; Moortgat, G. K. Gas-Phase Ozonolysis of Alkenes. Recent Advances in
430 Mechanistic Investigations. *Acc. Chem. Res.* **1998**, *31* (7), 387–396.
- 431 (13) Hellpointner, E.; Gäb, S. Detection of Methyl, Hydroxymethyl and Hydroxyethyl
432 Hydroperoxides in Air and Precipitation. *Nature* **1989**, *337* (6208), 631–634.
- 433 (14) O Dwyer, M. A.; Carey, T. J.; Healy, R. M.; Wenger, J. C.; Picquet-Varrault, B.; Doussin,
434 J. F. The Gas-Phase Ozonolysis of 1-Penten-3-Ol, (Z)-2-Penten-1-Ol and 1-Penten-3-One:
435 Kinetics, Products and Secondary Organic Aerosol Formation. *Z. Für Phys. Chem.* **2010**,
436 *224* (7–8), 1059–1080.
- 437 (15) Graedel, T. E. Terpenoids in the Atmosphere. *Rev. Geophys.* **1979**, *17* (5), 937.
- 438 (16) Grosjean, E.; Grosjean, D. Rate Constants for the Gas-Phase Reactions of Ozone with
439 Unsaturated Aliphatic Alcohols. *Int. J. Chem. Kinet.* **1994**, *26* (12), 1185–1191.
- 440 (17) Kalalian, C.; El Dib, G.; Singh, H. J.; Rao, P. K.; Roth, E.; Chakir, A. Temperature
441 Dependent Kinetic Study of the Gas Phase Reaction of Ozone with 1-Penten-3-Ol, Cis-2-
442 Penten-1-Ol and Trans-3-Hexen-1-Ol: Experimental and Theoretical Data. *Atmos. Environ.*
443 **2020**, *223* (October 2019), 117306.
- 444 (18) Gibilisco, R. G.; Bejan, I.; Barnes, I.; Wiesen, P.; Teruel, M. A. FTIR Gas Kinetic Study of
445 the Reactions of Ozone with a Series of Hexenols at Atmospheric Pressure and 298K. *Chem.*
446 *Phys. Lett.* **2015**, *618*, 114–118.
- 447 (19) Lin, X.; Ma, Q.; Yang, C.; Tang, X.; Zhao, W.; Hu, C.; Gu, X.; Fang, B.; Gai, Y.; Zhang,
448 W. Kinetics and Mechanisms of Gas Phase Reactions of Hexenols with Ozone. *RSC Adv.*
449 **2016**, *6* (87), 83573–83580.
- 450 (20) Grosjean, D.; Grosjean, E.; Williams, E. L. Rate Constants for the Gas-Phase Reactions of
451 Ozone with Unsaturated Alcohols, Esters, and Carbonyls. *Int. J. Chem. Kinet.* **1993**, *25* (9),
452 783–794.
- 453 (21) Atkinson, R.; Arey, J.; Aschmann, S. M.; Corchnoy, S. B.; Shu, Y. Rate Constants for the
454 Gas-Phase Reactions of Cis-3-Hexen-1-Ol, Cis-3-Hexenylacetate, Trans-2-Hexenal, and
455 Linalool with OH and NO₃ Radicals and O₃ at 296 ± 2 K, and OH Radical Formation Yields
456 from the O₃ Reactions. *Int. J. Chem. Kinet.* **1995**, *27* (10), 941–955.
- 457 (22) Chen, Y.; Wang, J.; Zhao, S.; Tong, S.; Ge, M. An Experimental Kinetic Study and Products
458 Research of the Reactions of O₃ with a Series of Unsaturated Alcohols. *Atmos. Environ.*
459 **2016**, *145*, 455–467.
- 460 (23) Li, W.; Chen, Y.; Tong, S.; Guo, Y.; Zhang, Y.; Ge, M. Kinetic Study of the Gas-Phase
461 Reaction of O₃ with Three Unsaturated Alcohols. *J. Environ. Sci.* **2018**, *71*, 292–299.
- 462 (24) Atkinson, R.; Carter, W. P. L. Kinetics and Mechanisms of the Gas-Phase Reactions of
463 Ozone with Organic Compounds under Atmospheric Conditions. *Chem. Rev.* **1984**, *84* (5),
464 437–470.
- 465 (25) Calvert, J. G.; Atkinson, R.; Kerr, J. A.; Madronich, S.; Moortgat, G. K.; Wallington, T. J.;
466 Yarwood, G. *The Mechanisms of Atmospheric Oxidation of the Alkenes*; Oxford University
467 Press, 2000.

- 468 (26) Pfrang, C.; King, M. D.; Braeckevelt, M.; Canosa-Mas, C. E.; Wayne, R. P. Gas-Phase Rate
469 Coefficients for Reactions of NO₃, OH, O₃ and O(³P) with Unsaturated Alcohols and Ethers:
470 Correlations and Structure-Activity Relations (SARs). *Atmos. Environ.* **2008**, *42* (13),
471 3018–3034.
- 472 (27) McGillen, M. R.; Archibald, A. T.; Carey, T.; Leather, K. E.; Shallcross, D. E.; Wenger, J.
473 C.; Percival, C. J. Structure–Activity Relationship (SAR) for the Prediction of Gas-Phase
474 Ozonolysis Rate Coefficients: An Extension towards Heteroatomic Unsaturated Species.
475 *Phys Chem Chem Phys* **2011**, *13* (7), 2842–2849.
- 476 (28) Szabo, E.; Tarmoul, J.; Tomas, A.; Fittschen, C.; Dobe, S.; Coddeville, P. Kinetics of The
477 •OH-Radical Initiated Reactions of Acetic Acid and Its Deuterated Isomers. **2009**, *96* (2),
478 299–309.
- 479 (29) Crunaire, S.; Tarmoul, J.; Fittschen, C.; Tomas, A.; Lemoine, B.; Coddeville, P. Use of Cw-
480 CRDS for Studying the Atmospheric Oxidation of Acetic Acid in a Simulation Chamber.
481 *Appl. Phys. B* **2006**, *85* (2–3), 467–476.
- 482 (30) Bouzidi, H.; Djehiche, M.; Coddeville, P.; Fittschen, C.; Tomas, A. Atmospheric Chemistry
483 of α -Diketones: Kinetics of C5 and C6 Compounds with Cl Atoms and OH Radicals. *Int. J.*
484 *Chem. Kinet.* **2017**, *49* (2), 112–118.
- 485 (31) Johnson, D.; Marston, G. The Gas-Phase Ozonolysis of Unsaturated Volatile Organic
486 Compounds in the Troposphere. *Chem. Soc. Rev.* **2008**, *37* (4), 699.
- 487 (32) Turnipseed, A. A.; Andersen, P. C.; Williford, C. J.; Ennis, C. A.; Birks, J. W. Use of a
488 Heated Graphite Scrubber as a Means of Reducing Interferences in UV-Absorbance
489 Measurements of Atmospheric Ozone. *Atmospheric Meas. Tech.* **2017**, *10* (6), 2253–2269.
- 490 (33) Peters, S.; Bejan, I.; Kurtenbach, R.; Liedtke, S.; Villena, G.; Wiesen, P.; Kleffmann, J.
491 Development of a New LOPAP Instrument for the Detection of O₃ in the Atmosphere.
492 *Atmos. Environ.* **2013**, *67*, 112–119.
- 493 (34) Roman, C.; Arsene, C.; Bejan, I. G.; Olariu, R. I. Investigations into the Gas-Phase
494 Photolysis and OH Radical Kinetics of Nitrocatechols: Implications of Intramolecular
495 Interactions on Their Atmospheric Behaviour. *Atmospheric Chem. Phys.* **2022**, *22* (4),
496 2203–2219.
- 497 (35) McGillen, M. R.; Carter, W. P. L.; Mellouki, A.; Orlando, J. J.; Picquet-Varrault, B.;
498 Wallington, T. J. Database for the Kinetics of the Gas-Phase Atmospheric Reactions of
499 Organic Compounds. *Earth Syst. Sci. Data* **2020**, *12* (2), 1203–1216.
- 500 (36) Treacy, J.; Curley, M.; Wenger, J.; Sidebottom, H. Determination of Arrhenius Parameters
501 for the Reactions of Ozone with Cycloalkenes. *J. Chem. Soc. - Faraday Trans.* **1997**, *93*
502 (16), 2877–2881.
- 503 (37) Calvert, J. G.; Orlando, J. J.; Stockwell, W. R.; Wallington, T. J. *The Mechanisms of*
504 *Reactions Influencing Atmospheric Ozone*; Oxford University Press: Oxford, UK, 2015.
- 505 (38) Buras, Z. J.; Elsamra, R. M. I.; Jalan, A.; Middaugh, J. E.; Green, W. H. Direct Kinetic
506 Measurements of Reactions between the Simplest Criegee Intermediate CH₂OO and
507 Alkenes. *J. Phys. Chem. A* **2014**, *118*, 1997–2006.
- 508 (39) McGillen, M. R.; Curchod, B. F. E.; Chhantyal-Pun, R.; Beames, J. M.; Watson, N.; Khan,
509 M. A. H.; McMahon, L.; Shallcross, D. E.; Orr-Ewing, A. J. Criegee Intermediate–Alcohol
510 Reactions, A Potential Source of Functionalized Hydroperoxides in the Atmosphere. *ACS*
511 *Earth Space Chem.* **2017**, *1* (10), 664–672.
- 512 (40) Gai, Y.; Ge, M.; Wang, W. Kinetics of the Gas-Phase Reactions of Some Unsaturated
513 Alcohols with Cl Atoms and O₃. *Atmos. Environ.* **2011**, *45* (1), 53–59.

- 514 (41) Treacy, J.; Hag, M. El; O'Farrell, D.; Sidebottom, H. Reactions of Ozone with Unsaturated
515 Organic Compounds. *Berichte Bunsenges. Für Phys. Chem.* **1992**, *96* (3), 422–427.
- 516 (42) Grosjean, E.; Grosjean, D. Rate Constants for the Gas-Phase Reaction of Ozone with 1,2-
517 Disubstituted Alkenes. *Int. J. Chem. Kinet.* **1996**, *28* (6), 461–466.
- 518 (43) Avzianova, E. V.; Ariya, P. A. Temperature-Dependent Kinetic Study for Ozonolysis of
519 Selected Tropospheric Alkenes. *Int. J. Chem. Kinet.* **2002**, *34* (12), 678–684.
- 520 (44) Leather, K. E.; McGillen, M. R.; Percival, C. J. Temperature-Dependent Ozonolysis
521 Kinetics of Selected Alkenes in the Gas Phase: An Experimental and Structure–Activity
522 Relationship (SAR) Study. *Phys. Chem. Chem. Phys.* **2010**, *12* (12), 2935.
- 523 (45) Mason, S. A.; Arey, J.; Atkinson, R. Rate Constants for the Gas-Phase Reactions of NO₃
524 Radicals and O₃ with C₆–C₁₄ 1-Alkenes and 2-Methyl-1-Alkenes at 296 ± 2 K. *J. Phys.*
525 *Chem. A* **2009**, *113* (19), 5649–5656.
- 526 (46) McGillen, M. R.; Carey, T. J.; Archibald, A. T.; Wenger, J. C.; Shallcross, D. E.; Percival,
527 C. J. Structure-Activity Relationship (SAR) for the Gas-Phase Ozonolysis of Aliphatic
528 Alkenes and Dialkenes. *Phys. Chem. Chem. Phys.* **2008**, *10* (13), 1757–1768.
- 529 (47) Dayan, U.; Ricaud, P.; Zbinden, R.; Dulac, F. Atmospheric Pollution over the Eastern
530 Mediterranean during Summer – a Review. *Atmospheric Chem. Phys.* **2017**, *17* (21), 13233–
531 13263.
- 532 (48) Lin, M.; Horowitz, L. W.; Payton, R.; Fiore, A. M.; Tonnesen, G. US Surface Ozone Trends
533 and Extremes from 1980 to 2014: Quantifying the Roles of Rising Asian Emissions,
534 Domestic Controls, Wildfires, and Climate. *Atmospheric Chem. Phys.* **17**, 2943–2970.
- 535 (49) Pfrang, C.; King, M. D.; Canosa-Mas, C. E.; Wayne, R. P. Structure–Activity Relations
536 (SARs) for Gas-Phase Reactions of NO₃, OH and O₃ with Alkenes: An Update. *Atmos.*
537 *Environ.* **2006**, *40* (6), 1180–1186. <https://doi.org/10.1016/j.atmosenv.2005.09.080>.
- 538 (50) Hein, R.; Crutzen, P. J.; Heimann, M. An Inverse Modeling Approach to Investigate the
539 Global Atmospheric Methane Cycle. *Glob. Biogeochem. Cycles* **1997**, *11* (1), 43–76.
- 540 (51) Shu, Y.; Atkinson, R. Atmospheric Lifetimes and Fates of a Series of Sesquiterpenes. *J.*
541 *Geophys. Res. Atmospheres* **1995**, *100* (D4), 7275–7281.
- 542 (52) Wingenter, O. W.; Kubo, M. K.; Blake, N. J.; Smith Jr., T. W.; Blake, D. R.; Rowland, F.
543 S. Hydrocarbon and Halocarbon Measurements as Photochemical and Dynamical Indicators
544 of Atmospheric Hydroxyl, Atomic Chlorine, and Vertical Mixing Obtained during
545 Lagrangian Flights. *J. Geophys. Res. Atmospheres* **1996**, *101* (D2), 4331–4340.
- 546 (53) Orlando, J. J.; Tyndall, G. S.; Ceazan, N. Rate Coefficients and Product Yields from
547 Reaction of OH with 1-Penten-3-Ol, (Z)-2-Penten-1-Ol, and Allyl Alcohol (2-Propen-1-Ol).
548 *J. Phys. Chem. A* **2001**, *105* (14), 3564–3569.
- 549 (54) Pfrang, C.; Baeza Romero, M. T.; Cabanas, B.; Canosa-Mas, C. E.; Villanueva, F.; Wayne,
550 R. P. Night-Time Tropospheric Chemistry of the Unsaturated Alcohols (Z)-Pent-2-En-1-Ol
551 and Pent-1-En-3-Ol: Kinetic Studies of Reactions of NO₃ and N₂O₅ with Stress-Induced
552 Plant Emissions. *Atmos. Environ.* **2007**, *41* (8), 1652–1662.
- 553 (55) Zhao, Z.; Husainy, S.; Smith, G. D. Kinetics Studies of the Gas-Phase Reactions of NO₃
554 Radicals with Series of 1-Alkenes, Dienes, Cycloalkenes, Alkenols, and Alkenals. *J. Phys.*
555 *Chem. A* **2011**, *115* (44), 12161–12172.
- 556 (56) Grira, A.; Amarandei, C.; Romanias, M. N.; El Dib, G.; Canosa, A.; Arsene, C.; Bejan, I.
557 G.; Olariu, R. I.; Coddeville, P.; Tomas, A. Kinetic Measurements of Cl Atom Reactions
558 with C₅–C₈ Unsaturated Alcohols. *Atmosphere* **2020**, *11* (3), 256.

- 559 (57) Rodríguez, A.; Rodríguez, D.; Garzón, A.; Soto, A.; Aranda, A.; Notario, A. Kinetics and
560 Mechanism of the Atmospheric Reactions of Atomic Chlorine with 1-Penten-3-Ol and (Z)-
561 2-Penten-1-Ol: An Experimental and Theoretical Study. *Phys. Chem. Chem. Phys.* **2010**,
562 *12* (38), 12245–12258.
- 563 (58) Gibilisco, R. G.; Santiago, A. N.; Teruel, M. A. OH-Initiated Degradation of a Series of
564 Hexenols in the Troposphere. Rate Coefficients at 298 K and 1 Atm. *Atmos. Environ.* **2013**,
565 *77*, 358–364.
- 566 (59) Davis, M. E.; Burkholder, J. B. Rate Coefficients for the Gas-Phase Reaction of OH with
567 (Z)-3-Hexen-1-Ol, 1-Penten-3-Ol, (E)-2-Penten-1-Ol, and (E)-2-Hexen-1-Ol between 243
568 and 404 K. *Atmospheric Chem. Phys.* **2011**, *11* (7), 3347–3358.
- 569 (60) Gibilisco, R. G.; Bejan, I.; Barnes, I.; Wiesen, P.; Teruel, M. A. Rate Coefficients at 298 K
570 and 1 Atm for the Tropospheric Degradation of a Series of C6, C7 and C8 Biogenic
571 Unsaturated Alcohols Initiated by Cl Atoms. *Atmos. Environ.* **2014**, *94*, 564–572.
- 572 (61) Gibilisco, R. G.; Blanco, M. B.; Bejan, I.; Barnes, I.; Wiesen, P.; Teruel, M. A. Atmospheric
573 Sink of (E)-3-Hexen-1-Ol, (Z)-3-Hepten-1-Ol, and (Z)-3-Octen-1-Ol: Rate Coefficients and
574 Mechanisms of the OH-Radical Initiated Degradation. *Environ. Sci. Technol.* **2015**, *49* (13),
575 7717–7725.
- 576 (62) Peirone, S. A.; Barrera, J. A.; Taccone, R. A.; Cometto, P. M.; Lane, S. I. Relative Rate
577 Coefficient Measurements of OH Radical Reactions with (Z)-2-Hexen-1-Ol and (E)-3-
578 Hexen-1-Ol under Simulated Atmospheric Conditions. *Atmos. Environ.* **2014**, *85*, 92–98.
- 579 (63) Jiménez, E.; Lanza, B.; Antiñolo, M.; Albaladejo, J. Photooxidation of Leaf-Wound
580 Oxygenated Compounds, 1-Penten-3-Ol, (Z)-3-Hexen-1-Ol, and 1-Penten-3-One, Initiated
581 by OH Radicals and Sunlight. *Environ. Sci. Technol.* **2009**, *43* (6), 1831–1837.
582

Table 1: Experimental results from the relative kinetic measurements employed in the present study for the ozonolysis of a series of alkenols.

Alcohol	OH scavenger	Reference	k/k_{ref}	$k \times 10^{17}$ ($\text{cm}^3 \text{ molecule}^{-1} \text{ s}^{-1}$)	k (average) $\times 10^{17}$ ($\text{cm}^3 \text{ molecule}^{-1} \text{ s}^{-1}$)
<i>trans</i> -2-hexen-1-ol	1,3,5-TMB	<i>trans</i> -2-butene	0.66±0.04	13.1±1.5	12.7±1.1
		cyclohexene	1.65±0.12	12.3±1.5	
<i>trans</i> -3-hexen-1-ol	1,3,5-TMB	<i>trans</i> -2-butene	0.24±0.02	4.84±0.62	5.01±0.30
		cyclohexene	0.74±0.04	5.49±0.62	
	cyclohexane	<i>trans</i> -2-butene	0.24±0.03	4.77±0.70	
		cyclohexene	0.65±0.08	4.86±0.74	
di-butyl ether	cyclohexene	0.67±0.08	4.98±0.75		
<i>cis</i> -3-hexen-1-ol	1,3,5-TMB	<i>trans</i> -2-butene	0.20±0.01	4.07±0.47	4.13±0.34
		cyclohexene	0.57±0.04	4.21±0.50	
<i>trans</i> -4-hexen-1-ol	1,3,5-TMB	<i>trans</i> -2-butene	0.71±0.05	14.1±1.7	14.0±1.2
		cyclohexene	1.87±0.16	13.9±1.8	



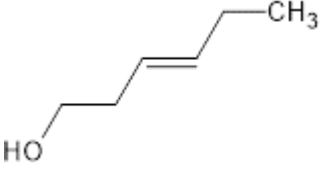
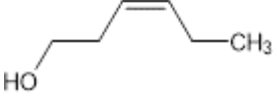
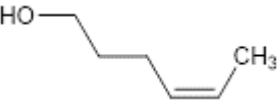
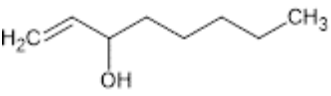

Table 2: Rate coefficients obtained in the present work using the absolute rate (pseudo first order) method (AR) and relative rate method (RR) compared with literature data.

Alcohol	$k \times 10^{17}$ (cm ³ molecule ⁻¹ s ⁻¹) ^a	Reference
<i>cis</i> -2-penten-1-ol	11.0±2.0 (AR)	This work
	16.9±2.5 (AR)	Grosjean and Grosjean ¹⁶
	11.5±0.7 (AR)	O'Dwyer et al. ¹⁴
	10.5±2.0 (RR)	Kalalian et al. ¹⁷
<i>trans</i> -2-hexen-1-ol	12.0±2.0 (AR)	This work
	12.7±1.1 (RR)	
	6.0±0.7 (RR)	Gibilisco et al. ¹⁸
<i>trans</i> -3-hexen-1-ol	16.6±2.2 (AR)	Lin et al. ¹⁹
	6.4±1.0 (AR)	This work
	5.01±0.30 (RR)	
	5.8±0.9 (RR)	Gibilisco et al. ¹⁸
<i>cis</i> -3-hexen-1-ol	6.2±0.7 (AR)	Lin et al. ¹⁹
	6.2±1.4 (RR)	Kalalian et al. ¹⁷
	5.8±0.9 (AR)	This work
	4.13±0.34 (RR)	
<i>cis</i> -3-hexen-1-ol	10.5±0.7 (AR)	Grosjean et al. ²⁰
	6.4±1.7 (RR)	Atkinson et al. ²¹
	6.0±0.9 (RR)	Gibilisco et al. ¹⁸
	5.5±0.7 (AR)	Lin et al. ¹⁹
	6.05±0.38 (RR)	Chen et al. ²²
	5.78±0.65 (AR)	
<i>trans</i> -4-hexen-1-ol	14.0±1.2 (RR)	This work
	10.5±1.4 (AR)	Lin et al. ¹⁹
1-octen-3-ol	2.0±0.3 (AR)	This work
	1.9±0.2 (AR)	Li et al. ²³

<i>trans</i> -2-octen-1-ol	8.4±1.3 (AR)	This work
----------------------------	---------------------	------------------

a: quoted uncertainties from the present work correspond to 2σ

Table 3: The comparison of different SAR methods and the ratio of $k_{\text{exp}}/k_{\text{SAR}}$. k_{exp} are the average of the absolute and relative rate coefficients obtained in the present work, where applicable.

Alcohol	k_{exp} (this work) ($\text{cm}^3 \text{ molecule}^{-1} \text{ s}^{-1}$)	k_{SAR} ($\text{cm}^3 \text{ molecule}^{-1} \text{ s}^{-1}$)	$k_{\text{SAR}}/k_{\text{exp}}$
 <i>cis</i> -2-penten-1-ol	1.10×10^{-16}	1.30×10^{-16} ^a	1.18
		1.20×10^{-16} ^b	1.09
		1.38×10^{-17} ^c	0.13
		1.08×10^{-16} ^d	0.98
 <i>trans</i> -2-hexen-1-ol	1.23×10^{-16}	2.00×10^{-16} ^a	1.61
		1.90×10^{-16} ^b	1.54
		1.38×10^{-17} ^c	0.11
		0.99×10^{-16} ^d	0.80
 <i>trans</i> -3-hexen-1-ol	5.71×10^{-17}	2.00×10^{-16} ^a	3.57
		1.90×10^{-16} ^b	3.33
		3.65×10^{-17} ^c	0.64
		2.80×10^{-17} ^d	0.49
 <i>cis</i> -3-hexen-1-ol	4.97×10^{-17}	1.30×10^{-16} ^a	2.63
		1.20×10^{-16} ^b	2.44
		3.68×10^{-17} ^c	0.74
		2.80×10^{-17} ^d	0.56
 <i>trans</i> -4-hexen-1-ol	1.40×10^{-16}	2.00×10^{-16} ^a	1.43
		1.90×10^{-16} ^b	1.35
		5.66×10^{-17} ^e	0.40
		4.11×10^{-17} ^d	0.29
 1-octen-3-ol	2.00×10^{-17}	1.20×10^{-17} ^a	0.60
		1.00×10^{-17} ^b	0.50
		3.72×10^{-18} ^c	0.19
		1.18×10^{-17} ^d	0.59
 <i>trans</i> -2-octen-1-ol	8.40×10^{-17}	2.00×10^{-16} ^a	2.38
		1.90×10^{-16} ^b	2.27

1.38×10^{-17} ^c	0.16
0.99×10^{-16} ^d	1.18

^a Atkinson and Carter²⁴, ^b Calvert et al.²⁵, ^c Pfrang et al.²⁶, ^d McGillen et al.²⁷, ^e Pfrang et al.⁴⁹ (for *trans*-4-hexen-1-ol, the OH group being far from the C=C double bond, the SAR from Pfrang et al.²⁶ for alkenols was not used but that developed for alkenes by Pfrang et al.⁴⁹).

Table 4: Comparison of atmospheric lifetimes of unsaturated alcohols with respect to removal by O₃, OH radicals, NO₃ radicals and Cl atoms. Average concentrations used: [O₃] = 1.6×10¹² molecules cm⁻³ ⁴⁷, [OH] = 2×10⁶ radicals cm⁻³ ⁵⁰, [NO₃] = 5×10⁸ radicals cm⁻³ ⁵¹, [Cl] = 10⁴ atoms cm⁻³ ⁵². Values in italic correspond to SAR calculations.

Alcohol	k _{O₃} (cm ³ molecule ⁻¹ s ⁻¹) <i>a</i>	τ _{O₃} (h)	k _{OH} (10 ⁻¹⁰ cm ³ molecule ⁻¹ s ⁻¹)	τ _{OH} (h)	k _{NO₃} (10 ⁻¹³ cm ³ molecule ⁻¹ s ⁻¹)	τ _{NO₃} (h)	k _{Cl} (10 ⁻¹⁰ cm ³ molecule ⁻¹ s ⁻¹)	τ _{Cl} (h)
<i>cis</i> -2-penten-1-ol	11.0	1.5	1.17 ^b	1.2	2.34 ^c	2.4	3.00 ^d	93
<i>trans</i> -2-hexen-1-ol	12.3	1.4	0.81 ^e	1.7	1.56 ^f	3.6	3.45 ^g	81
<i>trans</i> -3-hexen-1-ol	5.71	3.0	1.05 ^h	1.3	2.67 ^f	2.1	3.24 ^g	86
<i>cis</i> -3-hexen-1-ol	4.97	3.4	1.12 ⁱ	1.2	3.58 ^j	1.6	3.04 ^g	91
<i>trans</i> -4-hexen-1-ol	14.0	1.2	0.534 ^m	2.6	2.93 ^f	1.9	-	-
1-octen-3-ol	2.00	8.6	0.16 ⁿ	8.7	0.0099 ⁿ	560	4.03 ^k	69
<i>trans</i> -2-octen-1-ol	8.40	2.0	0.28 ⁿ	5.0	0.20 ⁿ	28	-	-

^a this work (average of absolute and relative determinations); ^b Orlando et al. ⁵³; ^c Average of Pfrang et al. ⁵⁴ and Zhao et al. ⁵⁵; ^d Average of Grira et al. ⁵⁶ and Rodriguez et al. ⁵⁷; ^e Average of Gibilisco et al. ⁵⁸ and Davis and Burkholder ⁵⁹; ^f Pfrang et al. ²⁶; ^g Average of Grira et al. ⁵⁶ and Gibilisco et al. ⁶⁰; ^h Average of Gibilisco et al. ⁶¹; Peirone et al. ⁶² and Gibilisco et al. ⁵⁸; ⁱ Average of Gibilisco et al. ⁵⁸, Jimenez et al. ⁶³, Atkinson et al. ²¹ and Davis and Burkholder ⁵⁹; ^j Average of Pfrang et al. ²⁶ and Atkinson et al. ²¹; ^k Grira et al. ⁵⁶; ^m Pfrang et al. ⁴⁹; ⁿ Pfrang et al. ²⁶; -: no data

Figures

Figure 1: Kinetic plot of *trans*-2-octen-1-ol ozonolysis.

Figure 2: Relative kinetic plot of ozone reaction with *trans*-2-hexen-1-ol versus (●) cyclohexene and (○) *trans*-2-butene, using 1,3,5-trimethylbenzene as OH scavenger.

Figure 3: Relationship between O₃ rate coefficient ratio and number of carbon atoms between -OH and C=C. For example, *cis*-2-penten-1-ol (OHCH₂-CH=CH-CH₂-CH₃) has one carbon atom between -OH and C=C. Stars (✱) represent data for 1-alken-3-ols (7 compounds) while circles (●) represent other alkenols (14 compounds). Rate coefficients for alkenes are from Calvert et al.²⁵ while those for alkenols are reported in Table S1.

Figure 4: Ozonolysis of alkenols: rate coefficients calculated by SAR (see McGillen et al.²⁷ and Supplementary Information) vs those determined experimentally at 298 K (see **Table S1**). The solid line is a linear regression over all the data (26 data) going through zero. The uncertainty on the slope corresponds to 2 standard deviations (2σ). One compound, 3-methyl-2-buten-1-ol, was excluded from the linear regression (see main text).

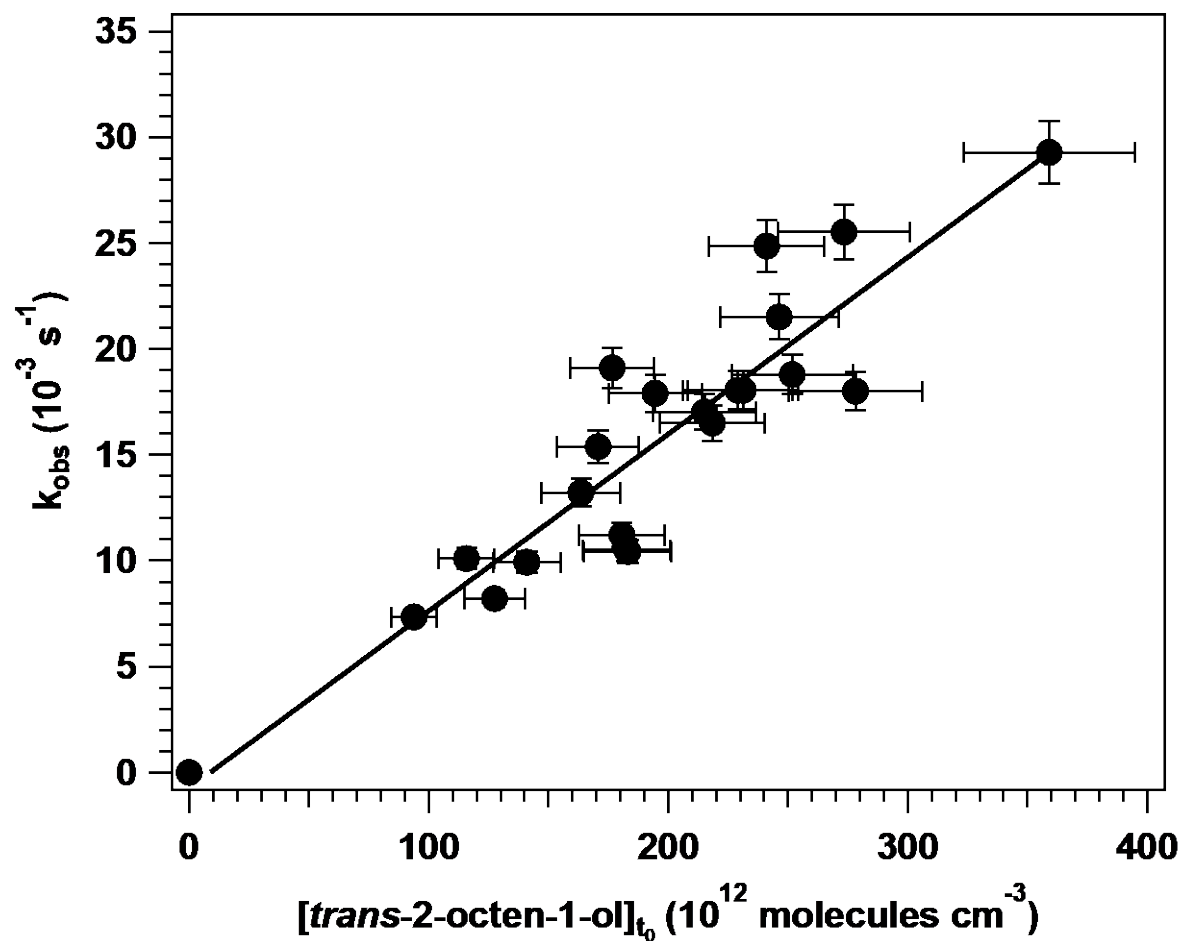


Figure 1: Kinetic plot of *trans*-2-octen-1-ol ozonolysis.

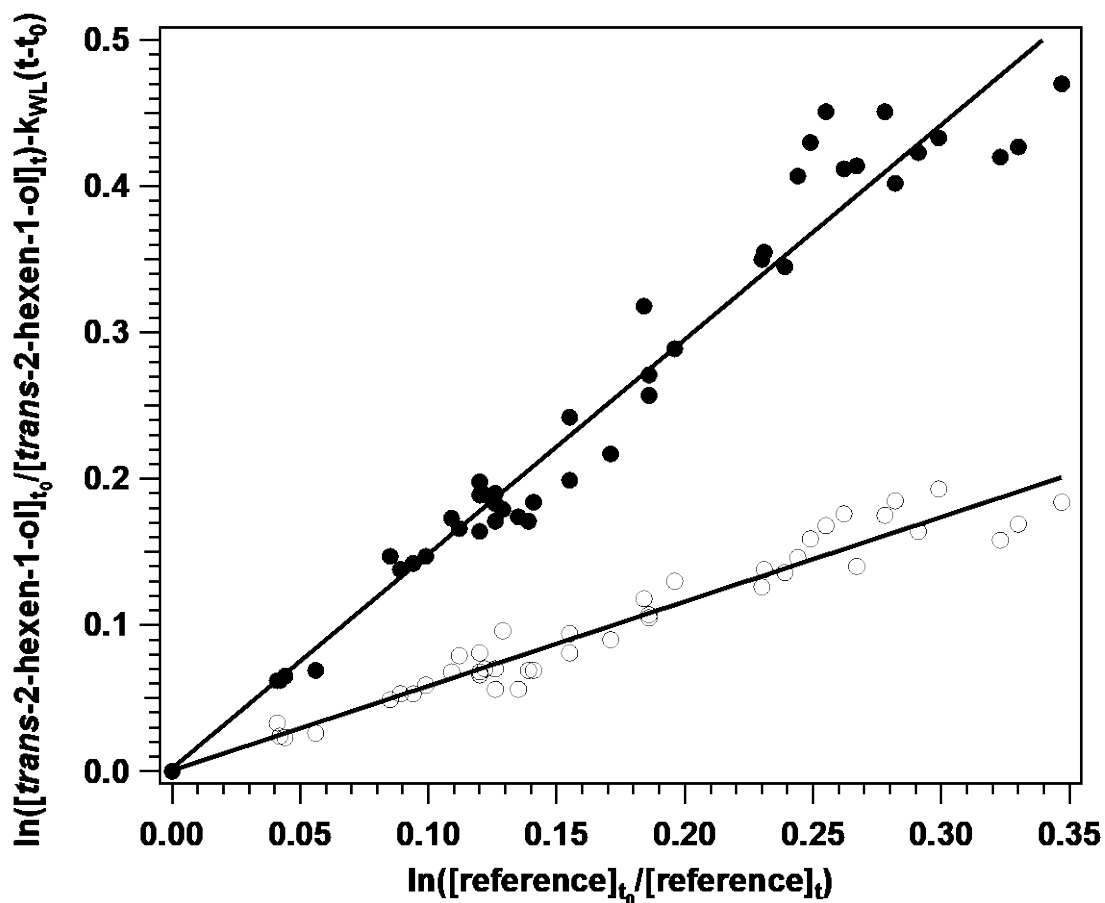


Figure 2: Relative kinetic plot of ozone reaction with *trans*-2-hexen-1-ol versus (●) cyclohexene and (○) *trans*-2-butene, using 1,3,5-trimethylbenzene as OH scavenger.

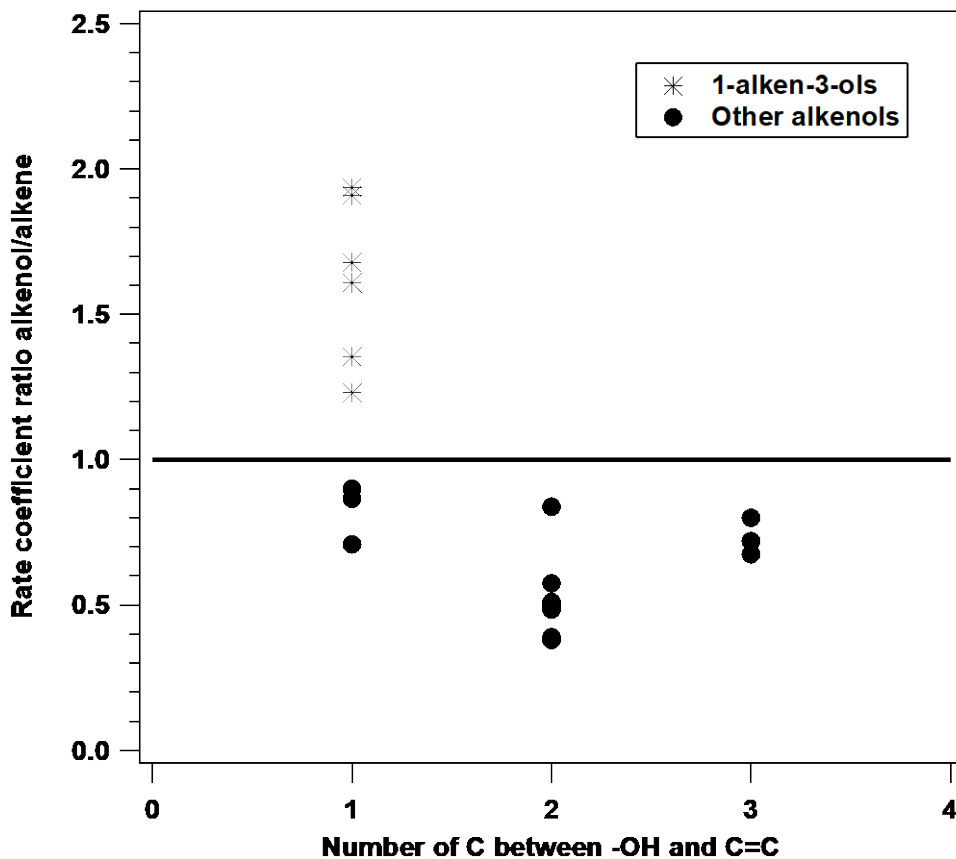


Figure 3: Relationship between O₃ rate coefficient ratio and number of carbon atoms between -OH and C=C. For example, *cis*-2-penten-1-ol (OHCH₂-CH=CH-CH₂-CH₃) has one carbon atom between -OH and C=C. Stars (*) represent data for 1-alken-3-ols (7 compounds) while circles (●) represent other alkenols (14 compounds). Rate coefficients for alkenes are from Calvert et al.²⁵ while those for alkenols are reported in Table S1.

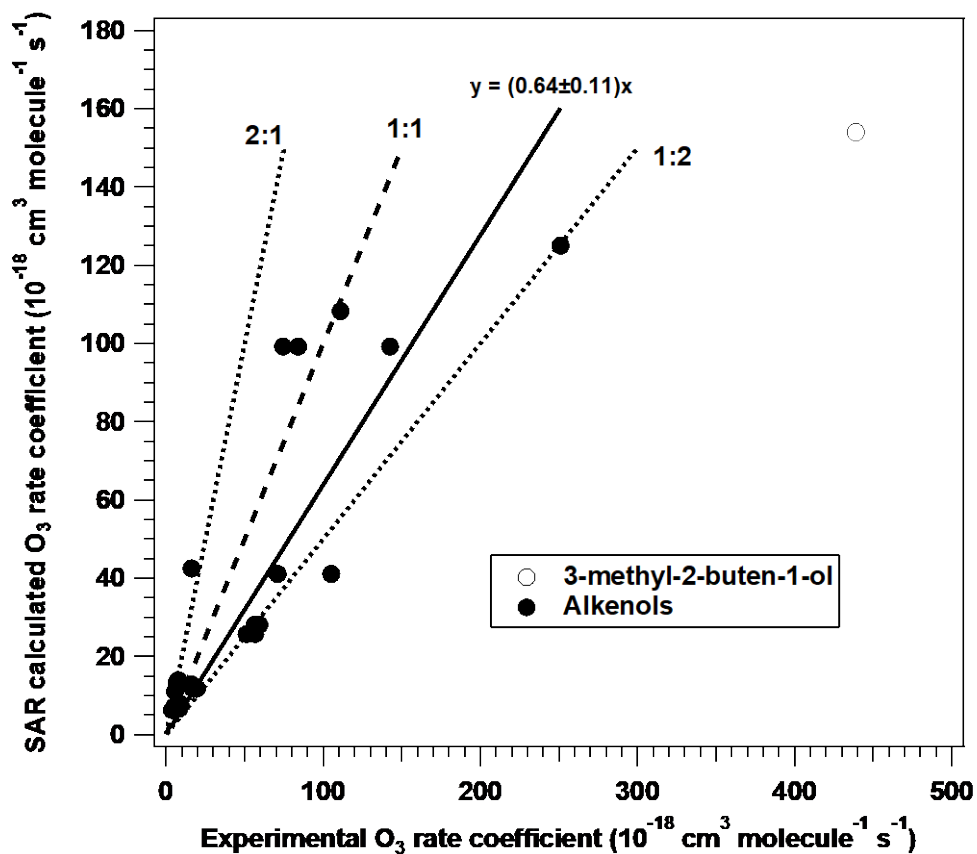


Figure 4: Ozonolysis of alkenols: rate coefficients calculated by SAR (see McGillen et al.²⁷ and Supplementary Information) vs those determined experimentally at 298 K (see **Table S1**). The solid line is a linear regression over all the data (26 data) going through zero. The uncertainty on the slope corresponds to 2 standard deviations (2σ). One compound, 3-methyl-2-buten-1-ol, was excluded from the linear regression (see main text).

TOC Graphic

